Journal of Physics: Conference Series **438** (2013) 012011 doi:10.1088/1742-6596/438/1/012011

# Plasmon excitations in photo- and electron impact ionization of fullerenes

**A V Verkhovtsev[1,2], A V Korol[1,3] and A V Solov'yov[1,4]**

[1] Frankfurt Institute for Advanced Studies, Ruth-Moufang-Str. 1, 60438 Frankfurt am Main, Germany

[2] St. Petersburg State Polytechnic University, Politekhnicheskaya ul. 29, 195251 St. Petersburg, Russia

[3] Department of Physics, St. Petersburg State Maritime Technical University, Leninskii prospekt 101, 198262 St. Petersburg, Russia

E-mail: verkhovtsev@fias.uni-frankfurt.de

**Abstract.** We study collective electron excitations (also referred to as plasmons) in the $C_{60}$ fullerene in the processes of photoionization and electron inelastic scattering. To reveal the contribution of collective electron excitations, we utilize the plasmon resonance approximation. It is shown that within this framework the photoionization cross section is described as a sum of two contributions, which represent two coupled modes of the surface plasmon. The electron energy loss spectra of $C_{60}$ are described by three contributions, namely by the two modes of the surface plasmon and the volume plasmon. The results of calculations are in good agreement with experimental data on photoionization and electron inelastic scattering of $C_{60}$. We show that the collective excitations play a significant role in the ionization process and provide a dominant contribution to the spectra.

## 1. Introduction

Since the discovery of fullerenes [1], the peculiar highly symmetric geometry and amazing properties [2] of these molecules have attracted a lot of interest and stimulated intensive experimental and theoretical investigations (see, e.g. [3]). At present, the investigation of fullerenes is active since they are proposed to be used in various fields of science and technology. For instance, excitation of fullerenes, placed in a biological medium, by an external radiation or incident heavy ions may lead to an enhancement in generation of secondary electrons or reactive oxygen species [4]. This allows fullerenes to be potentially used as sensitizers in photodynamic therapy or in ion-beam cancer therapy. A very important fundamental problem closely related to these application is an adequate description of dynamic response of fullerenes to external fields or to the interaction with projectiles.

A characteristic feature of a fullerene molecule is a partial delocalization of its electrons and hybridization of atomic orbitals. The valence $2s^2 2p^2$ electrons in each carbon atom form a cloud of delocalized electrons, which can be excited collectively by an external electric field. This excitation is represented as collective oscillation of delocalized electrons against the positively charged ions. By analogy with the collective electron excitations in condensed media, the collective excitations in fullerenes are referred to as plasmons.

[4] On leave from A.F. Ioffe Physical-Technical Institute, St. Petersburg, Russia

Content from this work may be used under the terms of the Creative Commons Attribution 3.0 licence. Any further distribution of this work must maintain attribution to the author(s) and the title of the work, journal citation and DOI.
Published under licence by IOP Publishing Ltd

It was predicted theoretically [5] and soon after observed experimentally [6] that the photoionization spectrum of the gas phase $C_{60}$ molecules is characterized by a broad prominent peak located at about 20 eV, the so-called giant resonance, which is formed due to collective electron excitations. Similar to photoionization, a broad resonant-like structure between 20 and 30 eV was observed in the process of inelastic scattering of electrons on $C_{60}$ [7–10]. Recent experiments on photoionization of neutral [11] and charged [12] $C_{60}$ molecules revealed the existence of the second collective resonance at about 40 eV and opened up the discussion [13,14] on the nature of this resonance.

In the present paper we study the formation of plasmon excitations in the $C_{60}$ fullerene in the processes of photoionization and electron inelastic scattering. To evaluate the contribution of collective electron excitations to the cross sections, we utilize the plasmon resonance approximation [15–17]. It allows one to apply the classical electrodynamics and hydrodynamics to study a collective motion of delocalized electrons of the system. We show that, similar to metal clusters [18], there are two different types of collective electron excitations, namely the surface and the volume plasmons, which can be formed in fullerenes. The dipole surface plasmon is responsible for the formation of the giant resonance in photoionization spectrum of fullerenes, while the volume plasmon modes, which have higher resonance frequencies, provide an essential contribution to the formation of the electron impact ionization cross section. Within the plasmon resonance approximation, the photoionization cross section of $C_{60}$ is described as a sum of two contributions, which represent two coupled modes of the surface plasmon. The electron energy loss spectra of fullerenes are described by three contributions, namely by the two modes of the surface plasmon and the volume plasmon as well. We show that the collective excitations play a significant role in the excitation process and provide a dominant contribution to the spectra.

The atomic system of units, $m = |e| = \hbar = 1$, is used throughout the paper.

## 2. Methods of investigation

To study the processes of photoionization and electron inelastic scattering from $C_{60}$, we utilize the following model. We consider the fullerene as a spherically symmetric system with a homogeneous charge distribution over the shell of a finite width, $\Delta R = R_2 - R_1$, where $R_{1,2}$ are the inner and the outer radii of the molecule, respectively [9, 19–21]. The chosen value of the shell's width, $\Delta R = 1.5$ Å, corresponds to the typical size of the carbon atom [20].

The equilibrium electron density distribution, $\rho_0(r)$, is expressed via the number $N$ of delocalized electrons (four valence $2s^2 2p^2$ electrons from each carbon atom, i.e. $N = 240$ in case of $C_{60}$) and the fullerene volume $V$:

$$\rho_0 = \begin{cases} N/V & \text{for } R_1 \le r \le R_2 \\ 0 & \text{if otherwise .} \end{cases} \tag{1}$$

The volume of the fullerene shell can be expressed as

$$V = \frac{4\pi}{3}\left(R_2^3 - R_1^3\right) = \frac{4\pi}{3} R_2^3 \left(1 - \xi^3\right) , \tag{2}$$

where $\xi = R_1/R_2 \le 1$ is the ratio of the inner to the outer radii. It should be mentioned that the spherical-shell model defined by equations (1) and (2) is applicable for any spherically symmetric system with an arbitrary value of the ratio $\xi$. Supposing $\xi = 0$, one obtains a model of a metal cluster [15,16,18], while the case $\xi = 1$ represents a fullerene modeled as an infinitely thin sphere [8, 15, 17].

Action of the external electric field causes variation of the electron density, $\delta\rho(r,t)$, in the system. Thus, the total electron density is introduced as

$$\rho(r,t) = \rho_0(r) + \delta\rho(r,t) , \tag{3}$$

where $\rho_0(r)$, defined by equation (1), denotes the stationary distribution of the negative charge.

Treating a collective motion of delocalized electrons of the system as a charged liquid, one can apply the classical electrodynamics and hydrodynamics to describe this motion. The detailed formalism of this approach is presented in [22–24]. Therefore, here we skip the details of the derivation and introduce the general equation for the variation of electron density in an arbitrary spherically symmetric system [23, 24]:

$$\Big(\omega^2 - 4\pi\rho_0(r)\Big)\delta\rho_l(r) + 4\pi\frac{\rho_0'(r)}{2l+1}\int_0^\infty g_l(r,r')\delta\rho_l(r')\mathrm{d}r' = q^2\rho_0(r)\phi_l(r) - \rho_0'(r)\phi_l'(r)\ , \qquad (4)$$

where $\delta\rho_l(r)$ is multipole variation of electron density in a spherically symmetric system under the action of the multipole component $\phi_l(r)$ of the external field, $\omega$ is the frequency of the external field, and the function $g_l(r,r')$ is defined as:

$$g_l(r,r') = l\left(\frac{r}{r'}\right)^{l-1}\Theta(r'-r) - (l+1)\left(\frac{r'}{r}\right)^{l+2}\Theta(r-r')\ , \qquad (5)$$

where $\Theta(x)$ is the Heaviside step function.

In case of the fullerene model defined above, the equilibrium electron density distribution, $\rho_0(r)$ (see equation (1)), and the corresponding derivative $\rho_0'(r)$ can be written as:

$$\rho_0(r) = \rho_0\,\Theta(r-R_1)\Theta(R_2-r)\ , \qquad \rho_0'(r) = \rho_0\Big(\delta(r-R_1) - \delta(r-R_2)\Big)\ , \qquad (6)$$

where $\delta(x)$ is the delta function.

The solution of equation (4) for a fullerene is then sought in the following form:

$$\delta\rho_l(r) = \delta\varrho_l(r)\Theta(r-R_1)\Theta(R_2-r) + \sigma_l^{(1)}\delta(r-R_1) + \sigma_l^{(2)}\delta(r-R_2)\ , \qquad (7)$$

where $\delta\varrho_l(r)$ describes the volume density variation arising inside the fullerene shell, and $\sigma_l^{(1,2)}$ are variations of the surface charge density at the inner and outer surfaces of the shell, respectively. The first term leads to the formation of the volume plasmon, while the two latter terms produce two coupled modes of the surface plasmon, the symmetric and antisymmetric ones [19, 20] (see figure 1).

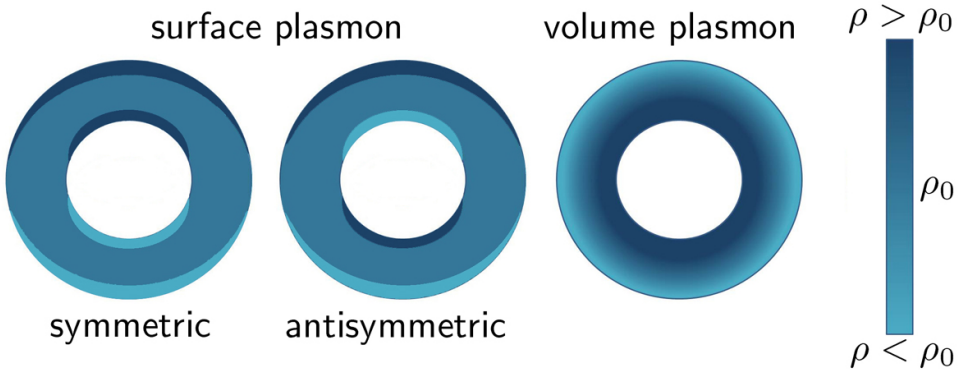


**Figure 1.** Representation of the two modes of the surface plasmon (left and middle panels) and of the volume plasmon (right panel). Light-blue and dark-blue regions represent the additional positive and negative charge, respectively.

The photoionization and inelastic scattering cross sections are treated within the plasmon resonance approximation [15–17]. It relies on the fact that collective plasmon excitations give the main contribution to the cross section in the vicinity of the giant resonance. A single-particle contribution, which comes from quantum phenomena, is not accounted for in the approximation, since the single-particle effects give a small contribution as compared to the collective modes [16, 18]. The detailed formalism for the description of plasmon excitations in electron- and photon-fullerene collisions is presented in [23, 24].

Within the plasmon resonance approximation, the differential inelastic scattering cross section of fast electrons in collision with fullerenes can be defined as a sum of three contributions:

$$\frac{\mathrm{d}^3\sigma}{\mathrm{d}\varepsilon_2\mathrm{d}\Omega_{\mathbf{p}_2}} = \frac{\mathrm{d}^3\sigma^{(v)}}{\mathrm{d}\varepsilon_2\mathrm{d}\Omega_{\mathbf{p}_2}} + \frac{\mathrm{d}^3\sigma^{(s_1)}}{\mathrm{d}\varepsilon_2\mathrm{d}\Omega_{\mathbf{p}_2}} + \frac{\mathrm{d}^3\sigma^{(s_2)}}{\mathrm{d}\varepsilon_2\mathrm{d}\Omega_{\mathbf{p}_2}} \ , \tag{8}$$

where

$$\begin{aligned}
\frac{\mathrm{d}^3\sigma^{(v)}}{\mathrm{d}\varepsilon_2\mathrm{d}\Omega_{\mathbf{p}_2}} &= \frac{2R_2p_2}{\pi q^4 p_1}\,\omega \sum_l \frac{\omega_p^2\,\Gamma_l^{(v)}\,V_l(q)}{\left(\omega^2-\omega_p^2\right)^2+\omega^2\Gamma_l^{(v)2}} \\
\frac{\mathrm{d}^3\sigma^{(s_1)}}{\mathrm{d}\varepsilon_2\mathrm{d}\Omega_{\mathbf{p}_2}} &= \frac{2R_2p_2}{\pi q^4 p_1}\,\omega \sum_l \frac{\omega_{1l}^2\,\Gamma_{1l}^{(s)}\,S_{1l}(q)}{\left(\omega^2-\omega_{1l}^2\right)^2+\omega^2\Gamma_{1l}^{(s)2}} \\
\frac{\mathrm{d}^3\sigma^{(s_2)}}{\mathrm{d}\varepsilon_2\mathrm{d}\Omega_{\mathbf{p}_2}} &= \frac{2R_2p_2}{\pi q^4 p_1}\,\omega \sum_l \frac{\omega_{2l}^2\,\Gamma_{2l}^{(s)}\,S_{2l}(q)}{\left(\omega^2-\omega_{2l}^2\right)^2+\omega^2\Gamma_{2l}^{(s)2}}
\end{aligned} \tag{9}$$

are obtained within the plane-wave first Born approximation. Here $\varepsilon_2 = \mathbf{p}_2^2/2$ is the kinetic energy of the scattered electron, $\Omega_{\mathbf{p}_2}$ its solid angle, $\mathbf{p}_1$ and $\mathbf{p}_2$ the initial and the final momenta of the projectile electron, $\mathbf{q} = \mathbf{p}_1 - \mathbf{p}_2$ the transferred momentum, $\omega = \varepsilon_1 - \varepsilon_2$ the energy loss, and $\varepsilon_1$ the kinetic energy of the incident electron. The volume plasmon frequency, $\omega_p = \sqrt{3N/(R_2^3 - R_1^3)}$ (where $N$ is the number of delocalized electrons), is related to the frequencies of the symmetric and antisymmetric surface plasmon modes of the multipolarity $l$ by the following expression [19, 20, 23]:

$$\omega_{(1,2)l}^2 = \frac{\omega_p^2}{2}\left(1 \mp \frac{1}{2l+1}\sqrt{1+4l(l+1)\xi^{2l+1}}\right) , \tag{10}$$

where the signs '−' and '+' correspond to the symmetric ($\omega_{1l}$) and the antisymmetric ($\omega_{2l}$) modes, respectively, and $\xi = R_1/R_2$. The quantities $\Gamma_l^{(v)}$ and $\Gamma_{jl}^{(s)}$ ($j = 1, 2$) are the widths of the plasmon resonances. Functions $V_l(q)$, $S_{1l}(q)$ and $S_{2l}(q)$ are the diffraction factors depending on the transferred momentum $q$. They determine the relative contribution of the multipole plasmon modes in various ranges of electron scattering angles and, thus, the resulting shape of the differential energy loss spectrum. Explicit expressions for these functions are given in [23].

It was shown [15] that the excitations with large angular momenta $l$ have a single-particle rather than a collective nature. It follows from the fact that with the increase of $l$ the wavelength of the plasmon excitation becomes smaller than the characteristic wavelength of the delocalized electrons in the fullerene. In the case of $C_{60}$, the estimates show [15] that the excitations with $l > 3$ are formed by single-electron transitions rather than by the collective excitations. Hence, only terms corresponding to the dipole ($l = 1$), quadrupole ($l = 2$) and octupole ($l = 3$) plasmon excitations should be accounted for in the sum over $l$ in equations (8) and (9).

The theory presented relies on the number of multipole terms to be accounted for ($l_{\max} = 3$) and the widths of the plasmon resonances, $\Gamma_{jl}^{(s)}$ and $\Gamma_l^{(v)}$, which are not just the fitting parameters

of the model but the real physical quantities. Their calculation can be performed considering another physical process, namely, the decay of the collective excitation mode into the incoherent sum of single-electron excitations. Such calculations are beyond the scope of the present paper. Nevertheless, one can estimate the widths of the plasmon excitations in the fullerene using the relation similar to the Landau damping of plasmon oscillations. Such an estimate results in $\Gamma_{jl}^{(s)} \sim l_{v_F}/\Delta R$, where $v_F$ is the velocity of the fullerene electrons on the Fermi surface. A similar estimate was successfully applied to the investigation of collective excitations in metal clusters [18].

In Ref. [13, 23, 24], it was shown that in case of photoionization, when the system interacts with a uniform external electric field, only the surface plasmon can occur. Indeed, the wave length of electromagnetic radiation is assumed to be much larger than the characteristic size of the system, i.e. the condition $\omega R \ll 1$ is fulfilled. This condition implies the validity of the dipole approximation, i.e. only dipole excitations ($l = 1$) may arise in the system due to interaction with the external electromagnetic field. In this limit, equation (4), describing interaction with an external field, is simplified due to $q = 0$. Thus, the photoionization cross section is defined as a sum of two contributions which correspond to the two modes of the surface plasmon [21, 23]:

$$\sigma(\omega) = \frac{4\pi\omega^2}{c}\left(\frac{N_1\,\Gamma_1}{\left(\omega^2-\omega_1^2\right)^2+\omega^2\Gamma_1^2}+\frac{N_2\,\Gamma_2}{\left(\omega^2-\omega_2^2\right)^2+\omega^2\Gamma_2^2}\right)\,. \tag{11}$$

Here $\omega$ is the photon energy, $\omega_1 \equiv \omega_{11}$ and $\omega_2 \equiv \omega_{21}$ are the frequencies of the symmetric and antisymmetric surface plasmon modes, respectively, $\Gamma_1 \equiv \Gamma_{11}^{(s)}$ and $\Gamma_2 \equiv \Gamma_{21}^{(s)}$ are the corresponding widths. $N_1$ and $N_2$ are the number of delocalized electrons, involved in each collective excitation, which should obey the sum rule $N_1 + N_2 = N$. The frequencies of the collective excitations are defined as [19–21]

$$\omega_{1,2}^2 = \omega_0^2 + \frac{\omega_p^2}{6}\left(3 \mp \sqrt{1+8\xi^3}\right)\,, \tag{12}$$

where the signs '−' and '+' correspond to the symmetric and antisymmetric modes, respectively, $\omega_p$ is the volume plasmon frequency defined above, and $\xi = R_1/R_2$. The term $\omega_0^2$ defines the free-electron picture threshold [20]. Following Ref. [20], we use the threshold value $\omega_0 = 14$ eV in the calculations. Below $\omega_0$, some of the electrons are treated as bound ones and, therefore, are not involved in the formation of the plasmon excitations.

In the calculations, we used the ratio $\gamma_1 = \Gamma_1/\omega_1 = 0.6$ for the symmetric mode, which corresponds to the experimental values obtained from the photoionization and energy loss experiments on neutral $C_{60}$ [6, 8]. For the antisymmetric mode, we used the value $\gamma_2 = \Gamma_2/\omega_2 = 1.0$ which corresponds to the widths of the second plasmon resonance obtained in the study of photoionization of $C_{60}^{q+}$ ($q = 1 - 3$) ions [12].

## 3. Results and discussion

In this section, we present the results of calculations of photo- and electron impact ionization spectra of the $C_{60}$ fullerene based on the formalism described above. Figure 2 represents the photoionization spectrum of $C_{60}$ calculated using the plasmon resonance approximation (see equation (11)). The left panel shows the spectrum obtained in the broad range of photon energies, namely up to 100 eV, while the right panel shows in more detail the region of the plasmon resonances, up to 50 eV. The symmetric and antisymmetric modes of the surface plasmon are shown by the dashed red and dash-dotted blue curves, respectively. The widths $\Gamma_1$ and $\Gamma_2$ of the symmetric and antisymmetric modes of the surface plasmon are equal to 11.4 and 33.2 eV, respectively, and correspond to the results of experimental measurements [6, 12]. The

sum of the two modes is shown by the thick solid green line. Theoretical curves are compared to the results of experimental measurements of photoabsorption of $C_{60}$ [6, 25, 26]. Open squares represent the recent compilation of experimental data made by Kafle *et al.* [25] in a broad energy range up to 100 eV (see the left panel). Open circles and stars represent, respectively, the compilation of experimental data made by Berkowitz [26] and the results of experimental measurements by Hertel *et al.* [6] (see the right panel).

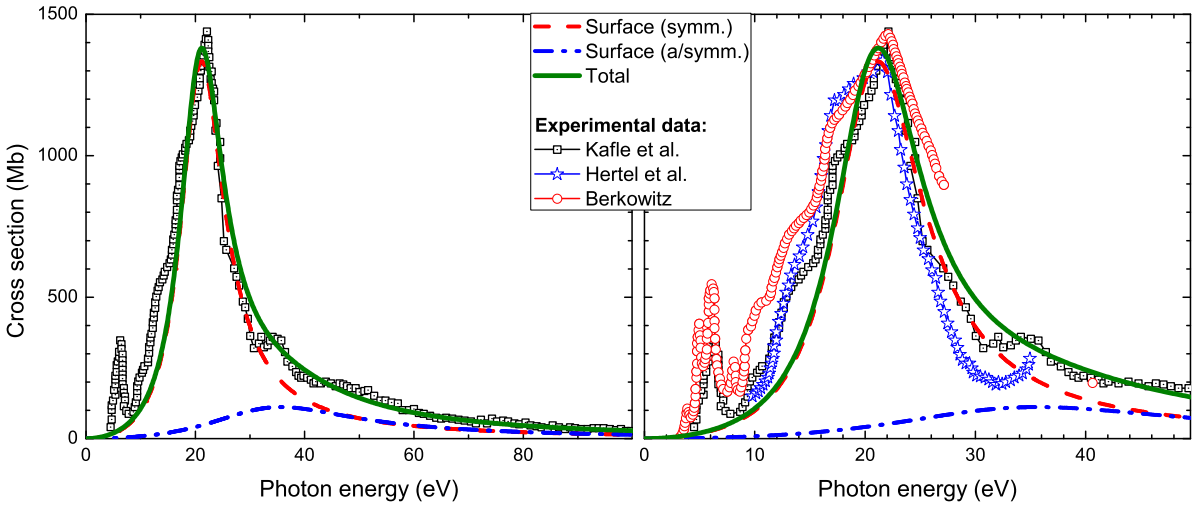


**Figure 2.** The photoabsorption cross section of $C_{60}$ calculated within the plasmon resonance approximation (thick green line). Contribution of the symmetric and antisymmetric modes of the surface plasmon are shown by the dashed red and dash-dotted blue lines, respectively. Theoretical curves are compared to the experimental data of Kafle *et al.* [25] (open squares), Berkowitz [26] (open circles) and Hertel *et al.* [6] (open stars). The left panel shows the spectrum obtained in the broad range of photon energies, up to 100 eV, and the right panel shows in more detail the region of the plasmon resonances, up to 50 eV.

As it is seen from figure 2, the plasmon resonance approximation gives a good agreement with the experimental data. The oscillator strength, calculated in the energy range up to 100 eV, is equal to 216.3, and corresponds to the experimentally measured value of 230.5 [25]. The plasmon resonance approximation describes quite well the main features of the giant resonance, such as height, width and position of the peak. Therefore, such a model can be considered as a useful tool for interpretation of experimental results. It should be also noted that the approach is focused on the study of collective electron excitations above the ionization threshold, which is about 7.6 eV for $C_{60}$ [6]. Therefore, it does not account for the series of discrete excitations, which manifest themselves in the low-energy region of the spectrum below 10 eV [27].

Figure 3 represents the electron energy loss spectra of $C_{60}$ calculated within the plasmon resonance approximation (see equations (8) and (9)). The calculations were performed for the scattering angles $\theta = 3°, 5°, 7°$ and $9°$, and the curves obtained were compared to the results of recent experimental measurements of the inelastic scattering of fast (1 keV) electrons on $C_{60}$ [9, 10]. The results of the comparison are presented in figure 3. For the sake of convenience, both the experimental and the theoretical curves are normalized to unity at the point of maximum.

Similar to the study of the photoionization process, we used the ratios $\gamma_{1l}^{(s)} = 0.6$ and $\gamma_{2l}^{(s)} = 1.0$ for the symmetric and antisymmetric modes, respectively. The widths of the volume

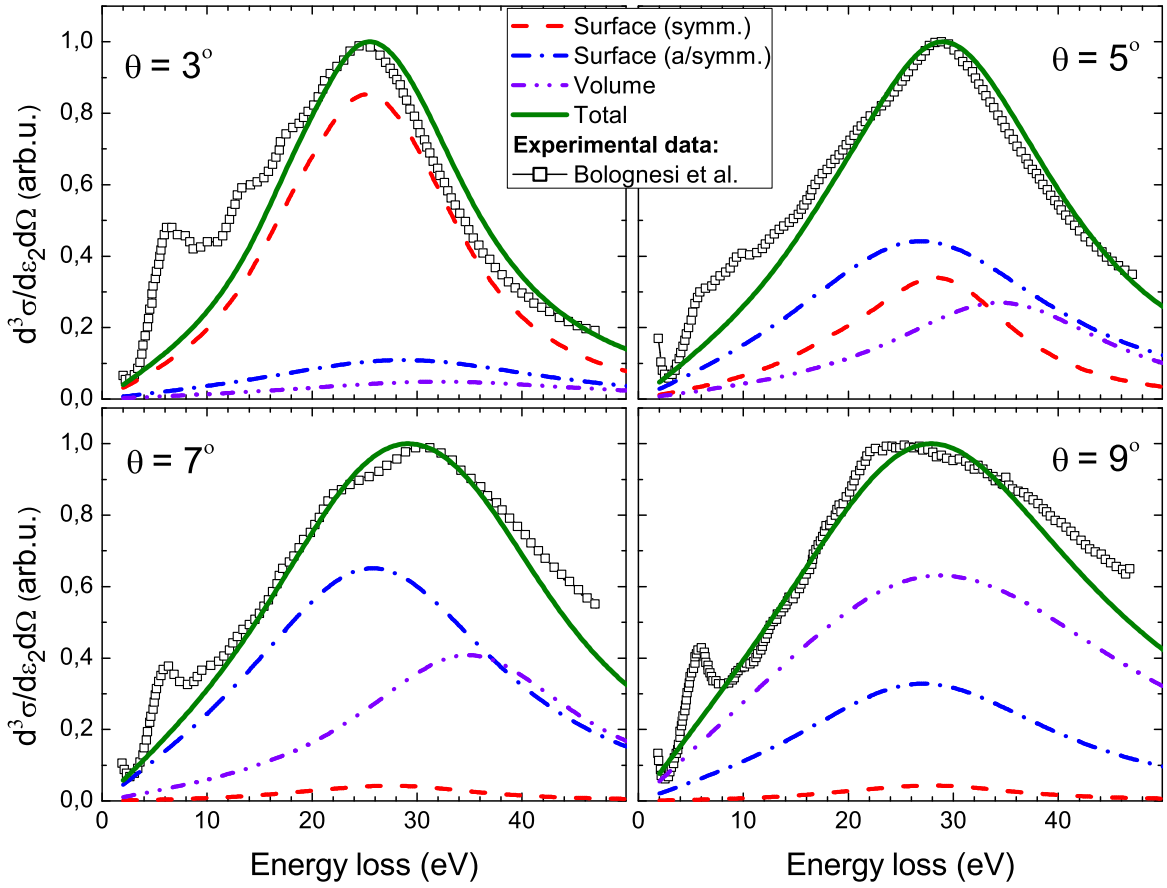


**Figure 3.** Comparison of the electron energy loss spectra, calculated within the plasmon resonance approximation, with the experimental spectra measured for the incident energy range 1002-1050 eV and for the scattering angles $\theta = 3^\circ \ldots 9^\circ$. The symmetric and antisymmetric modes of the surface plasmon are shown by dashed red and the dash-dotted blue lines, respectively; the volume plasmon contribution is shown by the double-dotted purple line. The total cross section is shown by the thick green line. Open squares represent the experimental data [9, 10]. For the sake of convenience, both the experimental and the theoretical curves are normalized to 1 at the point of maximum. The energy scale is the same for all panels.

plasmon were varied to obtain a better agreement with the experimental data. In the present calculations, the ratios $\gamma_l^{(v)} = \Gamma_l^{(v)}/\omega_p$ were considered within the range $0.7 \ldots 1.3$. The values of the plasmon frequencies and the corresponding widths for all three collective excitations are summarized in table 1.

In figure 3, the dashed red and dash-dotted blue curves represent, respectively, the symmetric and antisymmetric modes of the surface plasmon, the double-dotted purple line shows the contribution of the volume plasmon. The sum of the three collective excitations is shown by the thick green line. Open squares represent the experimental data [9, 10].

At the small scattering angle, $\theta = 3^\circ$, the symmetric mode of the surface plasmon (dashed red line) dominates the cross section. A similar behavior is observed in the photoionization process (see figure 2). In fact, in the case of the uniform external field ($q \to 0$), there is no volume plasmon excitation in the system and the symmetric plasmon mode exceeds significantly the antisymmetric mode. Non-uniformity of the external field causes the formation of the volume

**Table 1.** Peak positions and the widths of the two surface plasmon modes and of the volume plasmon used in the present calculations. All values are given in eV.

| | $l=0$ | $l=1$ | $l=2$ | $l=3$ |
|---|---|---|---|---|
| $\omega_{1l}$ | 0 | 19.0 | 25.5 | 30.5 |
| $\Gamma^{(s)}_{1l}$ | 0 | 11.4 | 15.3 | 18.3 |
| $\omega_{2l}$ | 37.1 | 33.2 | 31.0 | 29.5 |
| $\Gamma^{(s)}_{2l}$ | 37.1 | 33.2 | 31.0 | 29.5 |
| $\omega_p$ | | 37.1 | | |
| $\Gamma^{(v)}_{l}$ | | 26.0 - 48.3 | | |

plasmon whose contribution to the cross section is insignificant when the scattering angle is small. With increasing the scattering angle ($\theta = 5^\circ$ and $7^\circ$), the symmetric mode of the surface plasmon becomes less relevant and the antisymmetric mode (dash-dotted blue line) more prominent. At the larger angle ($\theta = 9^\circ$), the symmetric surface plasmon almost does not contribute to the cross section while the volume plasmon (double-dotted purple line) becomes dominant. The contribution of the antisymmetric surface and the volume plasmons can explain the origin of the two peaks in the energy loss range from 20 to 30 eV at the scattering angle $\theta = 7^\circ$.

The peak position of each plasmon resonance (9) as well as of the resulting cross section $\mathrm{d}^3\sigma/\mathrm{d}\varepsilon_2\mathrm{d}\Omega_{\mathbf{p}_2}$ is influenced by the manifestation of the diffraction effects. In Ref. [8], it was shown that plasmon modes with different angular momenta provide dominating contributions to the differential cross section at different scattering angles, which leads to the significant angular dependence of the energy loss spectrum. This phenomenon was described in terms of the electron diffraction at the fullerene edge [8]. As it is seen from equation (9), the resonance peak of each plasmon is defined not only by the plasmon frequencies $\omega_p$, $\omega_{1l}$ and $\omega_{2l}$ but also by the multipolar diffraction factors $V_l(q)$, $S_{1l}(q)$ and $S_{2l}(q)$ which depend on the transferred momentum $q$. In the limiting case of an infinitely thin layer, this dependence is described by the spherical Bessel functions $j_l^2(qR)$ which oscillate with $q$ and, thus, give suppression and enhancement of the partial plasmon modes at certain angles [8]. The incident energy of the projectile does not influence on this behavior and defines only the absolute value of the cross section.

## 4. Conclusion

To conclude, we studied the formation of plasmon excitations in the $C_{60}$ fullerene in the processes of photoionization and electron inelastic scattering. To reveal the contribution of collective electron excitations, we utilized the plasmon resonance approximation. We showed that the photoionization cross section of $C_{60}$ is described within the utilized approach as a sum of two contributions, which represent two coupled modes of the surface plasmon. In case of electron inelastic scattering, non-uniformity of the external electric field causes also the formation of the volume plasmon, whose contribution to the cross section is insignificant for small scattering angles and becomes dominant, as the angle increases. The results of calculations are in good agreement with experimental data on photoionization and electron inelastic scattering of $C_{60}$. The plasmon resonance approximation describes quite well the main features of the giant resonance, such as height, width and position of the peak as the model is proved to be a useful tool for interpretation of experimental results.

## References

[1] Kroto H W *et al* 1985 *Nature* **318** 162
[2] Hebard A F, Rosseinsky M J, Haddon R C, Murphy D W, Glarum S H, Palstra T T M, Ramirez A P and Kortan A R 1991 *Nature* **350** 600
[3] Sattler K D 2010 *Handbook of Nanophysics: Clusters and Fullerenes* (Boca Raton: CRC Press)
[4] Mroz P *et al* 2008 *Medicinal Chemistry and Pharmacological Potential of Fullerenes and Carbon Nanotubes* vol 1, ed F Cataldo and T Da Ros (New York: Springer Science+Business Media B.V.) p 79
[5] Bertsch G F, Bulgac A, Tomanek D and Wang Y 1991 *Phys. Rev. Lett.* **67** 2690
[6] Hertel I V, Steger H, de Vries J, Weisser B, Menzel C, Kamke B and Kamke W 1992 *Phys. Rev. Lett.* **68** 784
[7] Keller J W and Coplan M A 1992 *Chem. Phys. Lett.* **193** 89
[8] Gerchikov L G, Efimov P V, Mikoushkin V M and Solov'yov A V 1998 *Phys. Rev. Lett.* **81** 2707
[9] Verkhovtsev A V, Korol A V, Solov'yov A V, Bolognesi P, Ruocco A and Avaldi L 2012 *J. Phys. B: At. Mol. Opt. Phys.* **45** 141002
[10] Bolognesi P, Ruocco A, Avaldi L, Verkhovtsev A V, Korol A V and Solov'yov A V 2012 *Eur. Phys. J.* D **66** 254
[11] Reinköster A, Korica S, Prümper G, Viefhaus J, Godehusen K, Schwarzkopf O, Mast M and Becker U 2004 *J. Phys. B: At. Mol. Opt. Phys.* **37** 2135
[12] Scully S W J *et al* 2005 *Phys. Rev. Lett.* **94** 065503
[13] Korol A V and Solov'yov A V 2007 *Phys. Rev. Lett.* **98** 179601
[14] Scully S W J *et al* 2007 *Phys. Rev. Lett.* **98** 179602
[15] Gerchikov L G, Solov'yov A V, Connerade J-P and Greiner W 1997 *J. Phys. B: At. Mol. Opt. Phys.* **30** 4133
[16] Gerchikov L G, Ipatov A N and Solov'yov A V 1997 *J. Phys. B: At. Mol. Opt. Phys.* **30** 5939
[17] Gerchikov L G, Ipatov A N, Solov'yov A V and Greiner W 1998 *J. Phys. B: At. Mol. Opt. Phys.* **31** 3065
[18] Gerchikov L G, Ipatov A N, Polozkov R G and Solov'yov A V 2000 *Phys. Rev.* A **62** 043201
[19] Lambin Ph, Lucas A A and Vigneron J-P 1992 *Phys. Rev.* B **46** 1794
[20] Östling D, Apell P and Rosen A 1993 *Europhys. Lett.* **21** 539
[21] Lo S, Korol A V and Solov'yov A V 2007 *J. Phys. B: At. Mol. Opt. Phys.* **40** 3973
[22] Lundqvist S and March N H 1983 *Theory of the Inhomogeneous Electron Gas* (New York: Plenum Press)
[23] Verkhovtsev A V, Korol A V and Solov'yov A V 2012 *Eur. Phys. J.* D **66** 253
[24] Connerade J-P and Solov'yov A V 2002 *Phys. Rev.* A **66** 013207
[25] Kafle B P, Katayanagi H, Prodhan M, Yagi H, Huang C and Mitsuke K 2008 *J. Phys. Soc. Jpn.* **77** 014302
[26] Berkowitz J 1999 *J. Chem. Phys.* **111** 1446
[27] Saito S and Oshiyama A 1991 *Phys. Rev. Lett.* **66** 2637